Demonstration of the mass-producible feature of a Cs vapor microcell technology dedicated to miniature atomic clocks

R. Vicarini[a,b], V. Maurice[a], M. Abdel Hafiz[a], J. Rutkowski[a], C. Gorecki[a], N. Passilly[a], L. Ribetto[b], V. Gaff[b], V. Volant[b], S. Galliou[a], R. Boudot[a,*]

[a] *FEMTO-ST, CNRS, UBFC, ENSMM, 26 rue de l'Epitaphe 25030 Besançon, France*
[b] *Tronics Microsystems, 98 Rue du Pré de l'Horme, 38926 Crolles cedex, France*

Abstract

We report on the characterization of Cs vapor microcells based on pill dispensers and fabricated in a MEMS foundry according to a process compatible with mass-production. More than three quarters of cells from 6-inch wafers are successfully filled with Cs vapor. Various cells of a given wafer have been characterized using coherent population trapping (CPT) spectroscopy, demonstrating similar buffer gas (Ne) pressure with a standard deviation of about 2.5 % and CPT resonances with similar linewidth and contrast properties. In addition, frequency drifts mainly attributed to cell inner atmosphere variations have been investigated onto several cells over 250-500 hour measurements. The corresponding contribution at 1 day averaging time to a clock fractional frequency stability is estimated to be about 10^{-11} or lower. In a last section, the fractional frequency stability of a clock prototype using one fabricated Cs-Ne microcell is measured to be $2.5 \times 10^{-11}\ \tau^{-1/2}$ up to 200 s averaging time and better than 2×10^{-11} at 10^5 s. The clock frequency stability is mainly limited at short-term by the frequency-to-amplitude (FM-AM) noise conversion process and the laser amplitude (AM) noise. The mid-term stability is mainly affected by temperature-induced light shift effects. These performances tend to demonstrate that this vapor cell technology, compatible with mass-production,

*Corresponding author
Email address: rodolphe.boudot@femto-st.fr (R. Boudot)

is suitable for miniature quantum clocks or sensors.

Keywords: Atomic physics, Coherent population trapping, Alkaline vapor cells

1. Introduction

Time and frequency references play a fundamental role in a wide variety of fundamental physics experiments and applications of everyday life including telecommunication network synchronization, secure data transfer, satellite-based inertial navigation, geodesy or power distribution. The performances of all these systems are directly related to the level of fractional frequency stability of the local clock they use. Moreover, with the rapid increase in the use of portable battery-operated electronics and related technologies, such systems require low-cost, low-power, highly miniaturized and high-performance clocks that can be mass-produced and easily integrated into new instruments and devices.

Over the last decades, the progress of micro-electro-mechanical systems (MEMS) technologies and semiconductor diode lasers, combined with coherent-population trapping (CPT) physics [1], has allowed the development of chip-scale atomic clocks (CSACs). These frequency references, of great interest for many applications [2], combine a buffer-gas filled microfabricated alkali vapor cell, a vertical-cavity surface-emitting laser (VCSEL) and electronics, and deliver a signal with a fractional frequency stability almost two orders of magnitude better ($\approx 10^{-11}$ at 1 day integration) than widely-used quartz crystal oscillators for a similar size ($\approx 15\,\mathrm{cm}^3$) and power consumption ($\approx 150\,\mathrm{mW}$). The first CSAC prototype was demonstrated in NIST [3, 4] and has led later [5, 6] to the first commercially-available CSAC product proposed now by Microsemi [7]. Other projects towards the development of alternative industrial commercial CSACs at the horizon 2020 are still actively pursued in America, Europe and Asia [8, 9, 10, 11].

The heart of a CSAC is a microfabricated buffer-gas filled alkali vapor cell.

MEMS techniques have allowed to simplify and lower dramatically the cost of vapor cells by adopting a collective fabrication approach [12]. MEMS cells fabrication methods usually start with the structuration by deep reactive ion etching (DRIE) of a silicon cavity, which is subsequently sandwiched between two anodically-bonded glass wafers. If the cell fabrication is now widespread, a relatively large variety of solutions have been proposed to fill cells with alkali metal and buffer gas [13, 14, 15, 16, 17, 18, 19, 20, 21], with variable success. To our knowledge, the MEMS cell technology used in the Microsemi CSAC product [7] remains to date the unique MEMS cell technology actually embedded in an industrial miniature atomic clock. The absence of alternative industrial MEMS cell technologies highlights the difficulty to develop reliable and low drift MEMS vapor cells, compatible with mass production and fully suitable for miniature atomic clocks specifications.

In 2007, an original microcell technology based on post-sealing laser activation of a Cs pill dispenser has been proposed in FEMTO-ST [22]. The pill (trade name Cs/AMAX/Pill/1-0.6 from SAES Getters), placed in a dedicated Si cavity prior to the final cell sealing and stable up to 500 °C, allows to perform the anodic bonding process in optimal temperature and voltage conditions. A two-step anodic bonding procedure [23] is used in order to fill the cells at the wafer level with a well-controlled buffer gas pressure. This cell technology has been adopted recently in several academic groups for various activities including aging test measurements [24, 25], applications to cold-atom experiments [26] or the development of stabilized lasers [27]. Over the last 2 years, this cell technology has been transfered from FEMTO-ST towards Tronics Microsystems, a well-known MEMS foundry and manufacturer.

The present work, through various cell characterizations, aims at demonstrating the suitability and viability of this cell technology, compatible with mass-production, for miniature atomic clocks applications. In section 2, a brief description of the Cs cell technology development at Tronics facilities is reported. A CPT-based clock setup implemented for characterization of the fabricated microcells is also reported. Section 3 describes experimental results. Section

3.1 describes the characterization of several cells extracted from a single wafer using basic CPT spectroscopy. Section 3.2 reports on the investigation of frequency shifts induced by cell inner atmosphere variations in 5 Cs-Ne microcells taken from different wafers. In Section 3.3, the fractional frequency stability measurements of a CPT clock using a Cs-Ne vapor cell picked up randomly in a batch fabricated by Tronics. The measured clock Allan deviation is at the level of $2.5 \times 10^{-11}\ \tau^{-1/2}$ up to 200 s. The Allan deviation at 10^5 s, better than 2×10^{-11}, is in good agreement with laser power induced frequency shift effects.

2. Description of the cell technology and of the characterization setup

2.1. Cell technology

The Cs microcells have been batch fabricated at Tronics Microsystems. Following the developments conducted at FEMTO-ST, an industrial production line has been set up on 150 mm diameter silicon substrates. This technology allows for the fabrication of up to 500 microcells per wafer. Figure1(a) shows a photograph of a Cs cell wafer fabricated at Tronics Microsystems. Figure1(b) shows a single Cs microcell unit: the MEMS cell is similar to the design described in [23], i.e. the CPT chamber is 2 mm in diameter and 1.5 mm long.

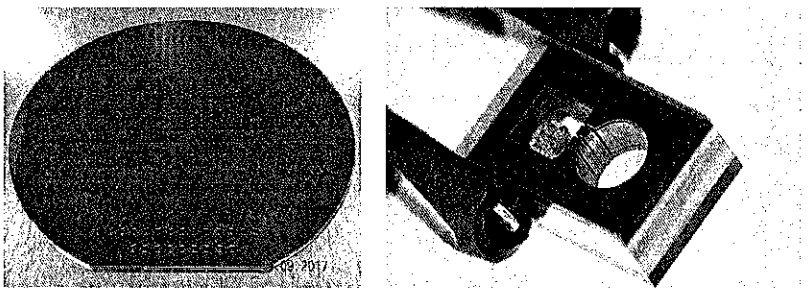

(a) (b)

Figure 1: Photographs of: (a) a 6-inch wafer of Cs cells microfabricated in Tronics Microsystems, and (b) a single Cs vapor cell unit where the pill dispenser is visible in the square-shaped cavity. The cylindrical cavity is the cavity where CPT interaction takes place.

In the process of industrialization, Tronics has improved DRIE etching and anodic bonding processes according to the microcell fabrication requirements, such as increased depth [28] and buffer gas environment [23]. The roughness of the cavity walls has been significantly lowered. The wafer bonding strength has been characterized and compares well to other published data [29]. The hermeticity of 25 microcells from 5 different batches was estimated with N_2O tests and no measurable leaks were observed with this method (the minimum detectable leak is equivalent to a He leak of 5×10^{-10} atm.cm^{3}s^{-1}).

A semi-automated setup, developed in FEMTO-ST and now available at Tronics, can be used for preliminary tests and qualification of MEMS Cs cells. This bench allows Cs dispenser activation at the wafer level of multiple buffer-gas filled MEMS cells using a high-power fibered laser. This setup also includes a linear spectroscopy setup used to confirm the presence of cesium vapor after the activation process and to estimate roughly the buffer gas pressure (uncertainty of a few torrs) in each cell unit of the wafer by measuring the buffer-gas induced optical frequency shift [30, 31] with respect to a reference evacuated cm-scale Cs cell. Out of the most recently fabricated wafers, 76 % of cells had a successful activation process and showed the presence of cesium vapor. A repeatable buffer gas pressure with a standard deviation of 3.3 % has been measured with this setup.

2.2. CPT clock-based characterization setup

A dedicated CPT clock-based setup, shown on Fig. 2, has been developed in order to characterize the batch-fabricated Cs cells. This setup can be used for basic CPT spectroscopy tests (Section 3.1), evaluation of the buffer gas pressure stability in the cell (Section 3.2) or to perform clock fractional frequency stability measurements (Section 3.3).

The laser source is a VCSEL produced by Vixar company and is tuned on the Cs D_1 line (894.6 nm) [32]. The VCSEL is modulated through a bias-tee with a 4.596 GHz microwave signal generated by a commercial frequency synthesizer

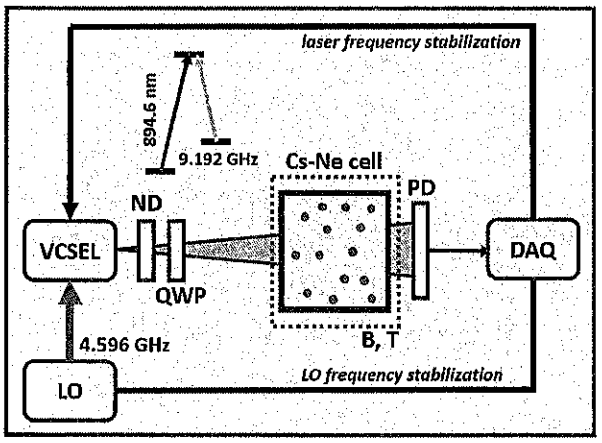

Figure 2: Simplified schematic of the CPT clock experimental setup. ND: neutral density filter, QWP: quarter wave plate, LO: local oscillator, PD: photodiode. The inset shows a simplified CPT energy diagram of the Cs atom involved in the experiment.

(Rohde-Schwarz SMB100A). This allows the generation of two first-order optical sidebands frequency-split by 9.192 GHz for CPT interaction. The laser beam is attenuated with a neutral-density filter and circularly polarized with a quarter-wave plate. For measurements of frequency drift induced by the cell inner atmosphere (Section 3.2), an acousto-optic modulator (not shown in Fig. 2) is inserted before the quarter wave-plate in order to control the laser power incident in the cell. The laser beam is finally sent through the Cs vapor cell before hitting a photodiode located at the cell output. The VCSEL beam diameter is about 2 mm in the cell. The cell is temperature-stabilized within the millikelvin level. A small solenoid applies a static magnetic field of 100 mG across the cell. The cell ensemble is surrounded by a mu-metal magnetic shield. The output signal of the photodiode is recorded by a data acquisition card, connected to a computer piloting most of the clock experiment. In clock configuration (Sections 3.2 or 3.3), the photodiode output signal is used in two servo loops. The first servo loop is dedicated to the laser frequency stabilization onto the bottom of a homogeneously broadened optical line. This is achieved through the use of a lock-in-amplifier system (Stanford Research SR830) applied onto the laser

DC current at a modulation frequency of 19 kHz. The second loop is used for stabilization of the local oscillator frequency onto the CPT resonance frequency. This servo uses a digital-based synchronous modulation-demodulation technique at 192 Hz. For clock frequency measurements, frequency variations of the output 4.596 GHz signal from the microwave synthesizer, piloted by a hydrogen maser, are recorded.

3. Experimental results

3.1. CPT spectroscopy and buffer gas pressure measurement

This section reports the characterization using CPT spectroscopy of five Cs-Ne microcells, noted 1 to 5, extracted from a single 6-inch wafer. The first objective is to determine the properties (linewidth and contrast) of the clock CPT resonance. Figure 3(a) shows an example of such a resonance detected in a microcell for an incident laser power of 39 µW. The full-width at half maximum (FWHM) of the resonance is 1838 Hz and the contrast C, defined as the CPT signal amplitude S divided by the DC background y_0, is 0.4 %.

The second objective is to estimate the actual buffer gas pressure in the cells through the measurement of the CPT resonance frequency. It is known indeed that the presence of buffer gas in a vapor cell causes a temperature-dependent frequency shift of the Cs clock transition [33]. The measurement methodology for the buffer gas pressure estimation is here briefly described. The measured clock frequency ν_c is assumed to be such that:

$$\nu_c = \nu_0 + \Delta\nu_z + \Delta\nu_I + \Delta\nu_{cell} \tag{1}$$

where ν_0 is the cesium atom unperturbed frequency (9 192 631 770 Hz), $\Delta\nu_z$ the Zeeman shift induced by the application of a static magnetic field B, $\Delta\nu_I$ the AC-stark light shift and $\Delta\nu_{cell}$ the shift induced by the cell temperature including the temperature dependent buffer gas pressure shift [33]. In our case, the contribution of $\Delta\nu_z \approx 427B^2 \approx 4.27$ Hz is minor and is neglected. The contribution of the AC Stark shift $\Delta\nu_I$ to the clock frequency is canceled by

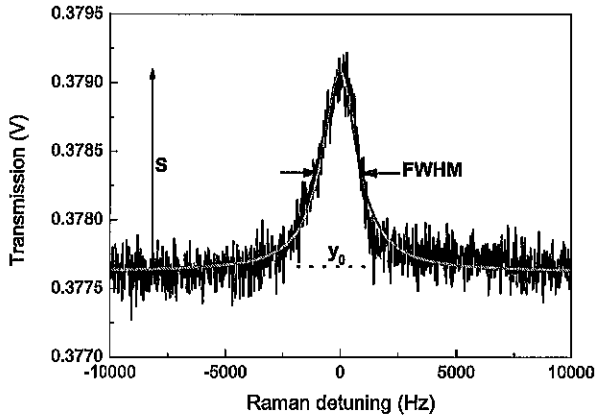

(a)

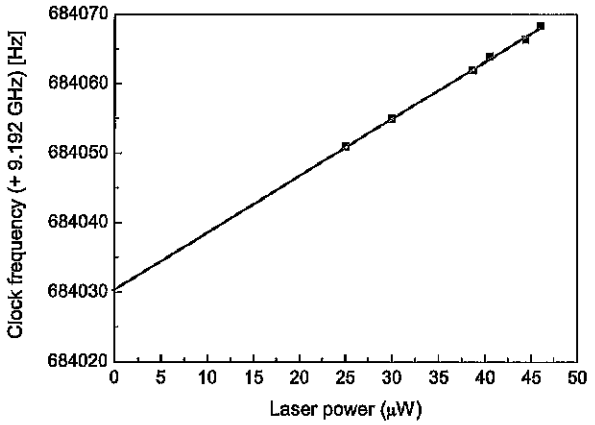

(b)

Figure 3: (a) CPT resonance detected in a Cs-Ne microcell (cell 1). The spectrum is fitted by a Lorentzian function. The cell temperature is 80 °C. (b) Measurement of the clock frequency versus the laser power (cell 1).

measuring the clock frequency at different optical power values and extrapolating it at null laser power using a linear fit function. The clock frequency is

concretely stabilized and averaged during about one minute for each value of the laser power P_L. Figure 3(b) shows such a measurement for the cell 1. The null-power clock frequency is measured to be 9 192 684 030 Hz in this case. The actual buffer gas pressure in the cell is then estimated from this value using Ne buffer gas collisional frequency shift coefficients reported in [33].

Table 1 details the main characteristics of cells 1 to 5. For each cell, the CPT resonance is measured for a cell temperature of 80 °C. The maximal deviation of the neon pressure is 1.9 Torr, i. e. about 2.5 % relative to the average pressure measured to be 76.1 Torr (at a reference temperature of 0 °C). The measured pressure is in correct agreement with the desired nominal pressure of 77 Torr at 0 °C. The characteristics of the CPT resonance detected in the 5 cells are also quite similar. CPT linewidths are found to be in the range from 1838 to 2118 Hz while CPT contrasts are all found between 0.39 and 0.5 %. This means that all these cells should allow the development of atomic clocks with similar short-term fractional frequency stability results. These preliminary results are satisfying and demonstrate the possibility to get on a single wafer, fabricated with industrial facilities, an ensemble of microcells with similar contents and CPT resonance characteristics.

3.2. Buffer gas pressure stability

It has been reported recently in the literature that the actual buffer gas pressure in microfabricated cells can drift slowly because of a gas permeation process through the cell windows, yielding a limitation to the clock long-term fractional frequency stability [24, 34, 25, 6]. In the present work, the CPT-clock based setup described in Section 2.2 is used to investigate frequency drifts related to buffer gas pressure changes in five different Cs-Ne microcells.

The measurement methodology described in [25] and inspired from section 3.1 is used. The measured clock frequency is given by Eq. 1. From measurements of both magnetic field and cell temperature fluctuations along time, respective contributions of these effects onto the clock frequency stability at 1 day averaging time are estimated to be negligible (see Section 3.3). The contribution of the

Table 1: Characteristics of 5 Cs-Ne microcells measured using CPT spectroscopy. All the cells were sealed in July 2016, activated in August 2016 and then stocked at ambient temperature. They were measured with the CPT setup in December 2017. CPT measurements are performed for a cell temperature of 80 °C. The clock frequency is the clock frequency extrapolated at null laser power (P_L=0). The measured Ne pressure is reported at a temperature of 0 °C and is estimated with an uncertainty of about ± 0.1 Torr.

Cell	FWHM (Hz)	C (%)	Clock frequency at $P_L = 0$ (Hz)	Ne pressure (Torr)
1	1838	0.4	9 192 684 030	75.0
2	1919	0.47	9 192 685 053	76.5
3	2118	0.39	9 192 685 290	76.9
4	2104	0.5	9 192 685 075	76.5
5	2024	0.49	9 192 684 344	75.5

AC Stark shift to the clock frequency is then canceled by regularly measuring the clock frequency at different optical power values and extrapolating it at null laser power using a linear fit function [25]. Variations of the null-power clock frequency, recorded along time, are then at the end expected to result mostly from the cell inner atmosphere variations. Note that, on the present setup, the only modification compared to [25] is that the laser power is now controlled and changed with an acousto-optic modulator (AOM) instead of a motorized rotating wave plate previously. We have checked that identical results were obtained in both cases for a given cell under test.

Buffer gas pressure variation-induced frequency drift measurements described in the following are delicate since environmental thermal effects and general agitation of the laboratory environment can jeopardize the mid-term frequency stability budget of the setup. We observed that the measured drift rate is in general reduced during quiet periods, such as the 2-weeks Christmas holidays where the laboratory is fully closed. Following measurements are performed with lab-scale electronics and external optics, cell after cell. In that sense, the present study aims at reporting preliminary results for a limited number of

cells and measured over a limited time duration. Figure 4 plots the extrapolated null-power clock frequency (in fractional value) versus time over 15-25 days measurements for five different cells. Four cells, noted a-b-2-4, are pill-dispenser based cells fabricated at Tronics. For comparison, one cell noted x, is a paste-dispenser cell similar to those described in [25]. Corresponding results are summarized in Table 2.

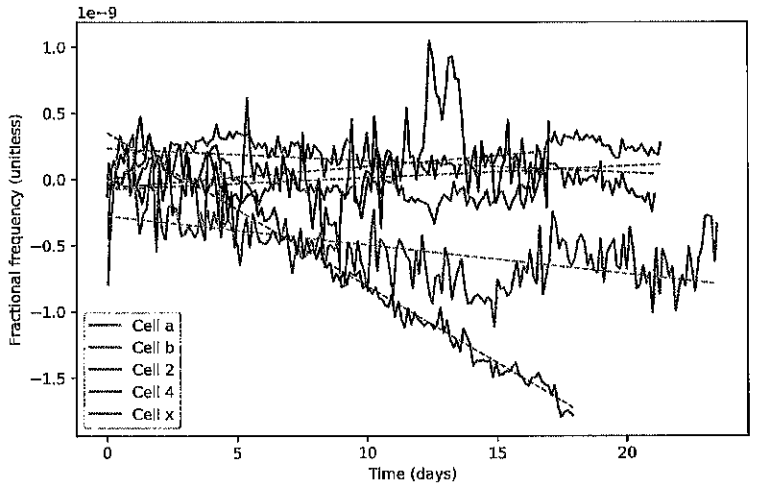

Figure 4: Evolution of the null-power clock frequency (in fractional value) versus time for five different cells. A linear extrapolation of a clock frequency-laser power dependence measurement is obtained roughly every 10 minutes. For clarity, the data is re-sampled and averaged over 3 hour periods. Null-power frequency data points are fitted by a linear function. Drift rate values are resumed in Table 2.

Reported results, possibly limited as explained above during some periods by ambient perturbations, present a non-negligible dispersion. For the cell a and x, the frequency drift rate is surprisingly measured to be positive, of about $+1 \times 10^{-11}$ per day. In this case, the positive sign of the drift cannot be the signature of a progressive reduction of the Ne buffer gas pressure in the cell. For all other tested cells, a negative frequency drift rate, that could result from a reduction of the buffer gas pressure, is obtained. All cells exhibit in absolute value a frequency drift rate close to 1×10^{-11} per day, which is acceptable for

Table 2: Investigations on clock frequency drifts induced by cell inner atmosphere evolution in 5 different Cs-Ne cells. Cells a, b, 2, 4 were fabricated at Tronics. The cell a, extracted from the wafer W_1, was sealed in May 2015, activated in August 2015 and started the aging test at 75 °C on June, 26 in 2017. The cell b, extracted from the wafer W_2, was sealed in May 2015, activated in August 2015 and started the aging test at 75 °C on July, 26 in 2017. Cells 2 and 4 were sealed in July 2016, activated in August 2016 and measured with the CPT setup in end 2017 and January 2018. The cell x, fabricated at FEMTO-ST, was sealed in July 2016, activated in August 2016 and started the aging test at 80 °C on June, 4 in 2017. All cells were basically stocked at ambient temperature between the Cs pill activation process and the beginning of the aging test. T_{cell} stands for the cell temperature. The measured Ne pressure is reported at a temperature of 0 °C and is estimated with an uncertainty of ± 0.1 Torr.

Cell	Wafer	T_{cell} (°C)	ν_c (Hz) (P_L =0)	P (Ne) (Torr)	Measurement duration (days)	Drift (10^{-11}/day)
a	W_1	75	9 192 682 352	72.6	17	+1.6
b	W_2	75	9 192 684 000	75.0	23	−2.18
2	W_3	80	9 192 685 053	76.5	21	−0.9
4	W_3	80	9 192 685 075	76.5	18	−11.5
x	W_4	80	9 192 672 639	58.8	21	+0.8

clock applications, except for the cell 4 for which a value of 1.15×10^{-10} per day is obtained. In other terms, at tested cell temperatures, 4 tested cells out of 5 exhibit performances compatible with miniature atomic clocks requirements. Reasons for failure of the cell 4 still need to be investigated. For last point, note that aging tests over about 200 days of miniature atomic clocks have been reported in [6]. In this article, a significant frequency drift of about -1×10^{-10} per day was obtained in early weeks before observation of a relevant reduction (about two orders of magnitude) of the frequency drift rate. In our case, cells were kept at ambient temperature and not ovenized between the date of their fabrication and the beginning of the aging test.

3.3. CPT clock frequency stability results

In this last section, a microcell fabricated in Tronics was used towards the development of a laboratory-prototype CPT clock, described in Fig. 2 and in Section 2.2. The cell is filled with a Ne buffer gas pressure of about 79 Torr and is temperature-stabilized at around 84 °C. Figure 5 shows the CPT resonance in clock configuration with optimized signal-to-noise ratio.

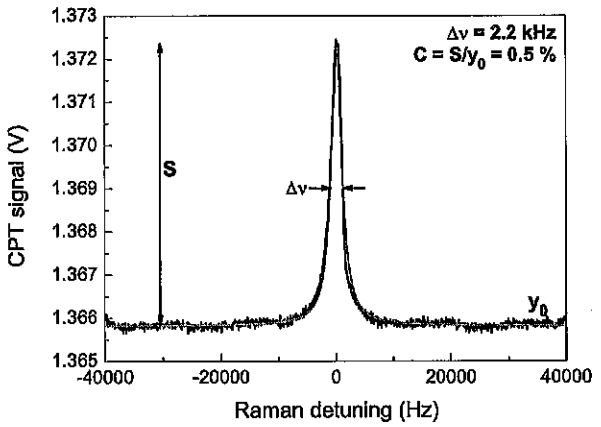

Figure 5: CPT resonance in clock configuration with optimized signal-to-noise ratio. Note also that the gain of the photodiode transimpedance amplifier is higher than for Fig. 3(a). The spectrum is fitted by a Lorentzian fit.

The CPT resonance FWHM is 2.2 kHz, with a contrast $C = S/y_0$ of 0.5 %, where S (6.7 mV) is the CPT resonance signal amplitude and y_0 the CPT DC background level (1.3658 V). The CPT resonance-based frequency discriminator slope is $3 \times 10^{-6}\,\mathrm{V\,Hz^{-1}}$.

We have measured the CPT resonance characteristics (FWHM, amplitude, contrast) versus several critical experimental parameters in order to optimize the clock short-term fractional frequency stability. Figures 6(a) and 6(b) plot the contrast/FWHM ratio of the CPT resonance versus the cell temperature and the laser power, respectively. This figure-of-merit is maximized for a cell temperature ranging from 75 to 85 °C and a laser power higher than 30 µW. In the

rest of the paper, the cell temperature is fixed at 84 °C and the laser power at the input of the cell is 31.5 µW. The resulting optical power at the cell output in the bottom of the absorption line where CPT takes place is about 19.5 µW (about 38 % of optical absorption).

Figure 7 shows the frequency shift of the clock transition (referred to 9.192 631 770 GHz) versus the total optical power illuminating the cell for several values of the microwave power out from the microwave synthesizer. For these measurements, the laser frequency is connected to the Cs atom $|F'\rangle = 3$ excited-state. Experimental data are fitted here by linear functions. It can be clearly seen that the light shift coefficient, i. e. the sensitivity of the clock frequency to laser power variations, can be greatly reduced and even annihilated at the first-order by tuning finely the microwave power. This behavior, explained by the dependence of the light shift coefficient on the CPT sidebands asymmetry, has already been observed in several references [35, 36, 37, 10]. In a recent paper, a mathematical formula was derived to calculate the light shift of a CPT spectral line produced and influenced by asymmetrical power distributions in the multi-chromatic laser field [38]. Here, for a microwave power value of about − 2 dBm, the light shift coefficient is reduced at a level of $-0.057\,\mathrm{Hz\,\mu W^{-1}}$ ($-6.2 \times 10^{-12}\,\mathrm{\mu W^{-1}}$ in fractional value at 9.192 GHz). The clock mid-term fractional frequency stability was found to be significantly improved by operating the clock close to this specific microwave power value.

Figure 8 plots the Allan deviation plot (all tau) of the CPT clock. This result is extracted from a 274-hour-long clock frequency measurement, with data points recorded every 0.1 s. The short-term fractional frequency stability is measured to be $2.5 \times 10^{-11}\ \tau^{-1/2}$ up to 200 s averaging time and below 3×10^{-12} at 1 hour integration time. Table 3 specifies the main contributions to the clock short-term frequency stability at $\tau = 1$ s. Contribution values were calculated from noise measurements (detector noise, laser AM noise and FM noise, local oscillator phase noise, etc.) performed on the experimental setup using expressions reported in [39]. The noise budget is in reasonable agreement (less than a factor 2) with the measured value at 1 s. The main contributions to the clock

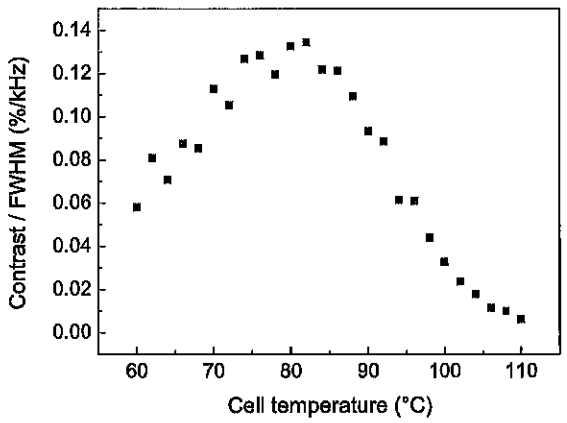

(a)

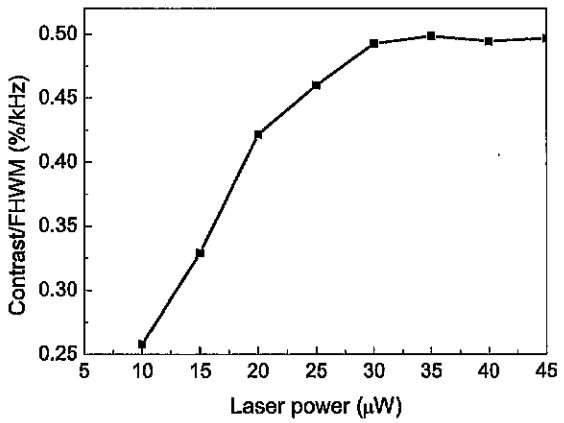

(b)

Figure 6: Contrast/FWHM ratio of the CPT resonance. (a) versus the cell temperature (for a laser power of 25 μW), (b) versus the laser power (for a cell temperature of 84 °C).

short-term frequency stability are the laser FM-AM noise conversion process and the laser AM noise. Other contributions are found to be at least one order of magnitude below.

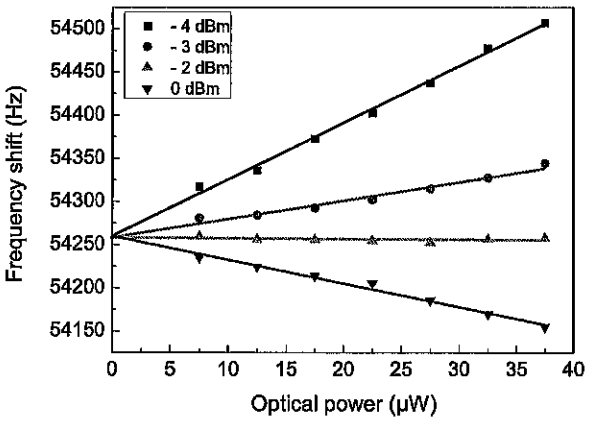

Figure 7: Frequency shift of the clock (refered to 9.192 631 770 GHz) versus the optical power incident in the cell for several values of the microwave power at the output of the synthesizer. The cell temperature is 84 °C.

For integration times longer than 1000 s, the clock Allan deviation is degraded to reach a level of 1.8×10^{-11} at 10^5 s averaging time. Table 4 details the mid-term stability budget of the clock at 10^5 s integration time. For this purpose, the sensitivity of the clock frequency to the main experimental parameters (laser power, laser frequency, cell temperature, magnetic field) and typical variations of these parameters at 10^5 s averaging time have been measured. The main limitation to the clock fractional frequency stability at 10^5 s is attributed to laser power-induced frequency shift effects, yielding a level of 1.8×10^{-11} at 10^5 s, in good agreement with the measured value shown on Fig. 8 (black curve). Other contributions reported in Table 4 are well below this level.

The clock Allan deviation at 10^5 s is reduced at 7×10^{-12} by applying a linear drift removal (-2.7×10^{-16} /s in fractional value) to frequency data. It is noted that the drift removal impacts the Allan deviation plot only for integration times higher than about 40 000 s. For time scales from 3000 to 40 000 s, the Allan deviation plot exhibits a strange $\approx 0.7\tau$ slope, neither the signature of a random-walk frequency noise (0.5 τ slope) nor a residual frequency drift

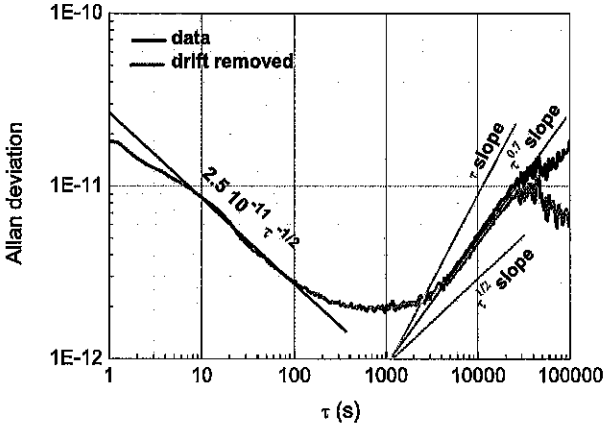

Figure 8: Allan deviation of the CPT clock, without (black line) or with (red line) drift removal. A thin blue solid line shows a $2.5 \times 10^{-11}\ \tau^{-1/2}$ dependence for the clock short-term fractional frequency stability. Thin solid lines with 0.5τ and τ slope functions are shown to highlight the 0.7τ slope (other blue solid line) of the Allan deviation in the 3000 - 40 000 s time range.

(τ slope), even with application of the drift removal. We suspect that the Allan deviation of the clock remains limited in this window by residual light-shift effects induced by a residual sensitivity of the laser system to the laboratory temperature variations. The sensitivity of the laser system to ambient temperature variations can induce along time laser power variations, laser frequency variations (expected however to be limited by the laser frequency servo loop) but also variations of the actual microwave power absorbed by the VCSEL since the VCSEL input impedance changes with its temperature [36].

We note also that the clock fractional frequency stability level of about 1.8×10^{-11} at 1×10^5 s is close to frequency drift values that could be attributed to buffer gas pressure variations as reported in section 3.2. Consequently, the evolution of the cell inner atmosphere is likely to contribute to the Allan deviation at 1×10^5 s and to the 0.7τ slope of the Allan deviation plot observed between 3000 and 40 000 s. The use of ASG wafers instead of borofloat glass wafers with

Table 3: Main contributions to the clock short term frequency stability at $\tau = 1$ s. The noise sources contributions are named and calculated as described in [39]. The local oscillator (LO) phase noise item describes the contribution of the LO phase noise to the clock Allan deviation through the intermodulation effect [40]. The laser AM-AM noise is the amplitude noise induced by the laser intensity noise. The laser FM-AM noise is the amplitude noise induced by the laser carrier frequency noise. Laser AM-FM and FM-FM are laser-induced frequency-shift effects from laser power and laser frequency variations respectively. Other contributions, from the cell temperature and magnetic field, are much lower.

Noise Source	σ (1 s)
Shot noise	8×10^{-13}
Detector noise	4×10^{-12}
LO phase noise	3×10^{-13}
Laser AM noise	2.3×10^{-11}
Laser FM-AM noise	3×10^{-11}
Laser AM-FM	3.6×10^{-12}
Laser FM-FM	2.3×10^{-12}
Cell temperature	3.8×10^{-12}
Magnetic field	2.6×10^{-14}
Total $\sigma_y(1s) = \sqrt{\sum \sigma_y^2}$	3.8×10^{-11}

Table 4: Main contributions to the clock mid-term frequency stability at $\tau = 10^5$ s. The evolution of the cell atmosphere is not considered here and is discussed in section 3.2.

Physical parameter	Sensitivity	Parameter Fluctuations	σ (10^5s)
Laser power	$3.6 \times 10^{-10}/\mu$W	5×10^{-8} W	1.8×10^{-11}
Laser frequency	2.3×10^{-18} / Hz	6×10^{5} Hz	1.3×10^{-12}
Cell temperature	3.8×10^{-10}/K	2.2×10^{-5} K	8.3×10^{-15}
Magnetic field	9.3×10^{-10}/G	1.1×10^{-5} G	1×10^{-14}
Total $\sigma_y(1s) = \sqrt{\sum \sigma_y^2}$	x	x	1.8×10^{-11}

present Cs-Ne cells could be a solution to investigate and study in the future to try to improve the cell inner atmosphere stability [34]. However, current results remain very encouraging towards the development of miniature atomic clocks.

4. Conclusions

We have reported characterizations of pill-dispenser based Cs microcells fabricated in industrial facilities, onto 6-inch wafers along a process compatible with mass production. Cell filling with Cs vapor by laser activation of the dispenser is successfully achieved for 76 % of cells. CPT spectroscopy was performed demonstrating among several cells from a given wafer a high buffer gas pressure homogeneity and similar CPT resonance properties (linewdith and contrast). The study of clock frequency drifts attributed to buffer gas pressure variations has been investigated onto several cell units. From these measurements, a typical average absolute frequency drift rate of about 1×10^{-11} per day is estimated as a reasonable value. A Cs-Ne microcell was used in a CPT atomic clock laboratory-prototype. The clock fractional frequency stability is 2.5×10^{-11}, 2×10^{-12} and 1.8×10^{-11} at 1 s, 1000 s and 10^5 s averaging time, respectively. The clock performances are limited at 1 s by the laser FM-AM conversion process and the laser AM noise. For times scales higher than 3000 s, the clock fractional frequency stability is expected to be limited by temperature-induced light-shift effects. The Allan deviation at 10^5 s is in good agreement with laser power-induced frequency shift effects. These results tend to demonstrate the viability of this MEMS cell technology for miniature quantum clocks.

Funding

Délégation Générale de l'Armement (DGA); Association Nationale de la Recherche et de la Technologie (ANRT).

Acknowledgments

R. Vicarini PhD thesis is funded by Tronics Microsystems and ANRT (CIFRE-Défense n° 11/2014/DGA). This work has been supported by DGA in the frame of Rapid HABAC project, Région de Franche-Comté and Labex FIRST-TF. We thank the platform Oscillator-Imp for the distribution of a reference hydrogen maser signal in the laboratory. The authors thank C. Rocher, P. Abbé and N. Vorobyev (FEMTO-ST) for their help with experimental work and electronics.

References

[1] J. Vanier, Atomic clocks based on coherent population trapping: a review, Applied Physics B 81 (2005) 421–442.

[2] E. Fernández, D. Calero, M. E. Parés, CSAC Characterization and Its Impact on GNSS Clock Augmentation Performance, Sensors 17 (2017).

[3] S. Knappe, V. Shah, P. D. D. Schwindt, L. Hollberg, J. Kitching, L.-A. Liew, J. Moreland, A microfabricated atomic clock, Applied Physics Letters 85 (2004).

[4] S. Knappe, MEMS atomic clocks, Comprehensive Microsystems 3 (2007) 571–612.

[5] R. Lutwak, A. Rashed, M. Varghese, G. Tepolt, J. LeBlanc, M. J. Mescher, D. K. Serkland, K. M. Geib, G. M. Peake, S. Römisch, The Chip-Scale Atomic Clock-Prototype Evaluation, in: Proceedings of the 39th Annual Precise Time and Time Interval Meeting, Long Beach, CA, 2007, pp. 269–290.

[6] R. Lutwak, A. Rashed, M. Varghese, G. Tepolt, J. Leblanc, M. J. Mescher, D. K. Serkland, G. M. Peake, The Miniature Atomic Clock - Pre-Production Results, 2007 IEEE International Frequency Control Symposium Joint with the 21st European Frequency and Time Forum (2007) 1327–1333.

[7] http://www.microsemi.com/products/timing-synchronization-systems/embedded-timing-solutions/components/sa-45s-chip-scale-atomic-clock (2018).

[8] S. Prazot, A. Stern, W. Israel, S. Marmor, C. Levi, I. Yevilevich, U. Arad, R. Man, B. Levi, The medium and long term stability of the nac atomic clock, in: 2017 Joint Conference of the European Frequency and Time Forum and IEEE International Frequency Control Symposium (EFTF/IFCS), 2017, pp. 162–168. doi:10.1109/FCS.2017.8088834.

[9] J. Haesler, L. Balet, S. Karlen, T. Overstolz, B. Gallinet, S. Lecomte, F. Droz, K. Kautio, P. Karioja, M. Lahti, A. Mttnen, O. Lahtinen, V. Hevonkorpi, Low-power and low-profile miniature atomic clock ceramic based flat form factor miniature atomic clock physics package (c-mac), in: 2017 Joint Conference of the European Frequency and Time Forum and IEEE International Frequency Control Symposium (EFTF/IFCS), 2017, pp. 55–56. doi:10.1109/FCS.2017.8088798.

[10] Y. Zhang, W. Yang, S. Zhang, J. Zhao, Rubidium chip-scale atomic clock with improved long-term stability through light intensity optimization and compensation for laser frequency detuning, J. Opt. Soc. Am. B 33 (2016) 1756–1763.

[11] Z. Zhang, R. Yang, X. Wang, The portable cpt atomic clocks - recent developments, in: 2017 Joint Conference of the European Frequency and Time Forum and IEEE International Frequency Control Symposium (EFTF/IFCS), 2017, pp. 605–606. doi:10.1109/FCS.2017.8088971.

[12] J. Kitching, S. Knappe, L. Hollberg, Miniature vapor-cell atomic-frequency references, Applied Physics Letters 81 (2002) 553–555.

[13] L.-A. Liew, S. Knappe, J. Moreland, H. G. Robinson, L. Hollberg, J. Kitching, Microfabricated alkali atom vapor cells, Applied Physics Letters 84 (2004) 2694–2696.

[14] S. Knappe, V. Gerginov, P. D. D. Schwindt, V. Shah, H. G. Robinson, L. Hollberg, J. Kitching, Atomic vapor cells for chip-scale atomic clocks with improved long-term frequency stability., Optics Letters 30 (2005) 2351–2353.

[15] Y. Pétremand, C. Affolderbach, R. Straessle, M. Pellaton, D. Briand, G. Mileti, N. F. de Rooij, Microfabricated rubidium vapour cell with a thick glass core for small-scale atomic clock applications, Journal of Micromechanics and Microengineering 22 (2012) 025013.

[16] L.-A. Liew, J. Moreland, V. Gerginov, Wafer-level filling of microfabricated atomic vapor cells based on thin-film deposition and photolysis of cesium azide, Applied Physics Letters 90 (2007) 114106.

[17] S. Woetzel, V. Schultze, R. IJsselsteijn, T. Schulz, S. Anders, R. Stolz, H.-G. Meyer, Microfabricated atomic vapor cell arrays for magnetic field measurements., The Review of scientific instruments 82 (2011) 033111.

[18] S. Karlen, J. Gobet, T. Overstolz, J. Haesler, S. Lecomte, Lifetime assessment of rbn3-filled mems atomic vapor cells with al2o3 coating, Opt. Express 25 (2017) 2187–2194.

[19] Y. Pétremand, C. Schori, R. Straessle, Low temperature indium-based sealing of microfabricated alkali cells for chip scale atomic clocks, Proc. European Frequency and Time Forum (EFTF) (2010) 2–4.

[20] R. Straessle, M. Pellaton, C. Affolderbach, Y. Pétremand, D. Briand, G. Mileti, N. F. de Rooij, Low-temperature indium-bonded alkali vapor cell for chip-scale atomic clocks, Journal of Applied Physics 6 (2013) 064501.

[21] S. Kang, R. P. Mott, K. A. Gilmore, L. D. Sorenson, M. T. Rakher, E. A. Donley, J. Kitching, C. S. Roper, A low-power reversible alkali atom source, Applied Physics Letters 110 (2017) 244101.

[22] A. Douahi, L. Nieradko, J. Beugnot, Vapour microcell for chip scale atomic frequency standard, Electronics Letters 43 (2007) 4–5.

[23] M. Hasegawa, R. K. Chutani, C. Gorecki, R. Boudot, P. Dziuban, V. Giordano, S. Clatot, L. Mauri, Microfabrication of cesium vapor cells with buffer gas for MEMS atomic clocks, Sensors and Actuators A: Physical 167 (2011) 594–601.

[24] S. Abdullah, C. Affolderbach, F. Gruet, G. Mileti, Aging studies on micro-fabricated alkali buffer-gas cells for miniature atomic clocks, Applied Physics Letters 106 (2015) 163505.

[25] V. Maurice, J. Rutkowski, E. Kroemer, S. Bargiel, N. Passilly, R. Boudot, C. Gorecki, L. Mauri, M. Moraja, Microfabricated vapor cells filled with a cesium dispensing paste for miniature atomic clocks, Applied Physics Letters 110 (2017) 164103.

[26] A. Dellis, S. Knappe, E. Donley, J. Kitching, Low he permeation cells for csacs, in: 8^{th} Frequency Standards and Metrology Symposium, 2015, p. 96.

[27] W. Loh, M. T. Hummon, H. F. Leopardi, T. M. Fortier, F. Quinlan, J. Kitching, S. B. Papp, S. A. Diddams, Microresonator brillouin laser stabilization using a microfabricated rubidium cell, Opt. Express 24 (2016) 14513–14524.

[28] R. K. Chutani, M. Hasegawa, V. Maurice, N. Passilly, C. Gorecki, Single-step deep reactive ion etching of ultra-deep silicon cavities with smooth sidewalls, Sensors and Actuators A: Physical 208 (2014) 66–72.

[29] A. Cozma, B. Puers, Characterization of the electrostatic bonding of silicon and pyrex glass, Journal of Micromechanics and Microengineering 5 (1995) 98.

[30] G. A. Pitz, D. E. Wertepny, G. P. Perram, Pressure broadening and shift of the cesium D_{1} transition by the noble gases and N_{2} , H_{2} , HD, D_{2} , CH_{4} , C_{2}H_{6} , CF_{4} , and ^{3}He, Physical Review A 80 (2009) 1–8.

[31] G. A. Pitz, C. Fox, G. P. Perram, Pressure broadening and shift of the cesium D_{2} transition by the noble gases and N_{2}, H_{2}, HD, D_{2}, CH_{4}, C_{2}H_{6}, CF_{4}, and ^{3}He with comparison to the D_{1} transition, Physical Review A 82 (2010) 1–9.

[32] E. Kroemer, J. Rutkowski, V. Maurice, R. Vicarini, M. A. Hafiz, C. Gorecki, R. Boudot, Characterization of commercially available vertical-cavity surface-emitting lasers tuned on cs d1 line at 894.6 nm for miniature atomic clocks, Appl. Opt. 55 (2016) 8839–8847.

[33] O. Kozlova, S. Guérandel, E. De Clercq, Temperature and pressure shift of the Cs clock transition in the presence of buffer gases: Ne, N_2, Ar, Physical Review A 83 (2011) 62714.

[34] A. T. Dellis, V. Shah, E. A. Donley, S. Knappe, J. Kitching, Low helium permeation cells for atomic microsystems technology, Opt. Lett. 41 (2016) 2775–2778.

[35] M. Zhu, L. S. Cutler, Theoretical and experimental study of light shift in a CPT-based Rb vapor cell frequency standard, 32nd Annual Precise Time and Time Interval (PTTI) Meeting (2000) 311–323.

[36] V. Shah, V. Gerginov, P. D. D. Schwindt, S. Knappe, L. Hollberg, J. Kitching, Continuous light-shift correction in modulated coherent population trapping clocks, Applied Physics Letters 89 (2006) 151124.

[37] D. Miletic, C. Affolderbach, M. Hasegawa, R. Boudot, C. Gorecki, G. Mileti, AC Stark-shift in CPT-based Cs miniature atomic clocks, Applied Physics B (2012).

[38] Y. Yin, Y. Tian, Y.-C. Wang, S.-H. Gu, The light shift of a chip-scale atomic clock affected by asymmetrical multi-chromatic laser fields, Spectroscopy Letters 50 (2017) 227–231.

[39] P. Yun, F. m. c. Tricot, C. E. Calosso, S. Micalizio, B. François, R. Boudot, S. Guérandel, E. de Clercq, High-performance coherent population trap-

ping clock with polarization modulation, Phys. Rev. Applied 7 (2017) 014018.

[40] B. Franois, C. E. Calosso, J. M. Danet, R. Boudot, A low phase noise microwave frequency synthesis for a high-performance cesium vapor cell atomic clock, Review of Scientific Instruments 85 (2014) 094709.

VITAE

Abstract

Vitae from the authors of the manuscript entitled :
Demonstration of the mass-producible feature of a Cs vapor microcell technology dedicated to miniature atomic clocks

Include in the manuscript a short (maximum 100 words) biography of each author.

Rémy Vicarini received his engineering diploma from ENSMM in Besançon, France. Specialized in mechanics and microtechnology, he is pursuing his Ph.D. at the FEMTO-ST Institute, in collaboration with Tronics Microsystems company. His PhD thesis deals with the design, development and test of a miniaturized physics package for a CPT atomic clock.

Vincent Maurice received his Ph.D. degree in 2016 from Université de Franche-Comté, Besançon, France. He is now working as a post-doctoral researcher at NIST, Boulder, in the Atomic Devices and Instrumentation (ADI) Group. His research interest includes microfabricated atomic clocks and frequency standards.

Moustafa Abdel Hafiz received his Ph.D. degree in 2017 from Université Bourgogne-Franche-Comté, Besançon, France. His thesis was about the development of a high performance microwave atomic clock based on CPT. He is now working as a post-doctoral researcher at PTB, Braunschweig, Germany, with the Yb^+ ion clock team.

Jaroslaw Rutkowski worked at CEA-Leti in Grenoble, France from 2011 to 2014. He received his Ph.D. from Université de Franche-Comté, Besançon, France in 2014. His thesis concerned the development of a miniature atomic magnetometer for space applications. He joined FEMTO-ST in 2015 as a post-doctoral researcher where he worked on the development of MEMS atomic clocks. Currently he holds the position of a Research engineer at Hertz Systems Ltd, Zielona-Gora, Poland where he works on Satellite Navigation Systems.

Christophe Gorecki is a Director of Research CNRS (DR1 CNRS) at FEMTO-ST. He received the Ph.D. in Optics at the University of Besançon in 1983 and joined Laboratoire d'Optique P.M. Duffieux (LOPMD) as a CNRS Scientist. His research interests included optical inspection and micro-measurements, applications of image processing techniques in optical metrology and Optical Pattern Recognition methods. From 1995 to 1998 he joined for 3 years the University of Tokyo where he was involved in research and development of Optical MEMS. Back to LOPMD he conducts research in novel MOEMS architectures for on-chip optical microscopy, the atomic micro-clocks as well as development of metrology methods for characterization of MOEMS/MEMS. C. Gorecki has more than 180 technical papers to his credit and 3 book chapters. From 1992 to 1995 C. Gorecki served as national Secretary of the French Society of Optics (SFO). He is also a Fellow of the SPIE and member of the Board of Directors of SPIE. From 2007 to 2009, Dr. Gorecki was a member and expert of Disciplinary Committee of French ANR for programs Blanc and Jeunes Chercheurs. He received in 2012 the prize of European Optical Society. He is the President of the Collégium SMYLE which is a virtual French-Swiss research laboratory including FEMTO-ST and EPFL Lausanne.

Nicolas Passilly is Senior Researcher at CNRS. He received his M.S. degree in physics and his Ph.D. degree in laser physics from the University of Caen, France, in 2002 and 2005, respectively. From 2006 to 2008, he was post-doctoral researcher at the University of Eastern Finland, Joensuu, Finland. In 2008, he

joined FEMTO-ST Institute, Besançon, France, and became CNRS scientist in 2010. His research interest includes micro-optics and MOEMS devices.

Luca Ribetto received his M.S. degree in Micro and Nano Technologies from Politecnico di Torino, Grenoble INP and Ecole Polytechnique Fédérale de Lausanne (EPFL) in 2008. He obtained his Ph.D. degree in Microtechnologies from EPFL in 2012. He currently works at Tronics Microsystmes, as Product Development Engineer and has been in charge of the projects on chip-scale atomic clocks since 2014.

Vincent Gaff is Business Unit Manager (Microsystems Solutions) at Tronics Microsystems. He manages the contract development and manufacturing activities of the company since 2010. He joined TRONICS in 1999 as Marketing and Sales Engineer and then served as Business Development Manager from 2006 to 2010. He was previously at CEA-Leti marketing department where he worked as consultant for Tronics and Thales Avionics in the frame of Europractice, an access action of the European Commission.

Valérie Volant was Senior packaging process Engineer at Tronics Microsystems from 2010 to 2017. She was in charge of all Tronics assembly and packaging activities. She had previously worked during 10 years as a packaging process engineer and then as back-end process supply team manager for CMOS image sensors for space applications at Atmel and then e2v. She currently works on Packaging and assembly development at Isorg.

Serge Galliou is full-time senior Professor at ENSMM/FEMTO-ST, Univ. Bourgogne Franche Comté, France. Research interests include topics such as precise temperature control, low phase noise electronics, design of various types of crystal oscillators and more recently chip scale atomic clocks, investigations on behavior of BAW resonators (quartz and langatate) at liquid helium temperature and optomechanics related applications. He managed the team Piezo-

electric Resonators and Ultrastable Oscillators from 2001 to 2007, and also especially initiated works on cryogenic acoustic resonators in 2005. Presently he is deputy director of the Time and Frequency department after being at its head during two years.

Rodolphe Boudot received his M.S. degree and his Ph.D. degree in engineering sciences, in 2003 and 2006 respectively, both from Université de Franche-Comté, Besançon, France. From 2007 to 2009, R. Boudot was post-doctoral researcher at the Systèmes de Références Temps-Espace laboratory (SYRTE, Paris, France. Since October 2008, R. Boudot has been a permanent CNRS researcher at FEMTO-ST. His research interests include compact and miniature vapor cell atomic clocks, low noise electronics, oscillators and frequency synthesizers, laser spectroscopy and more recently cold-atom experiments.